

# ESTIMATION OF ACOUSTIC FIELD IN 1-D DUCT USING ARTIFICIAL NEURAL NETWORKS

**Anonymous authors**

Paper under double-blind review

## ABSTRACT

1 Estimation of sound field in one-dimension finds extensive applications in many  
2 areas such as speech, automotive, aerospace and biomedical industries. Tradition-  
3 ally, it is obtained by solving Helmholtz equation using analytical and numerical  
4 methods (finite difference, finite element, etc.). This paper discusses a neural  
5 network methodology to solve 1-D Helmholtz equation subjected to some con-  
6 straints. Unlike other governing equations, Helmholtz equation poses a biasing  
7 problem with the loss functions at higher frequencies. In the current work, an au-  
8 tomatic weight update algorithm is proposed to bypass this difficulty. The results  
9 obtained from the proposed methodology are compared with those of the analyti-  
10 cal method. A good correlation has been observed between the two methods. The  
11 robustness of the methodology with respect to the frequency is also verified.

## 12 1 INTRODUCTION

13 In many engineering applications, sound propagation is dominant in one-dimension(Munjal, 2014).  
14 For instance, in the modelling and analysis of speech, automotive intake/exhaust sounds, human  
15 respiratory sounds, etc., the acoustic field variation is primarily significant in the direction of largest  
16 dimension as compared to the other directions. In those cases, 1-D Helmholtz equation with appro-  
17 priate boundary condition will provide an acoustic field distribution required to perform the intended  
18 study. Traditionally, this task is performed by means of analytical(Veerababu & Venkatesham, 2020;  
19 2021) and numerical methods(Ihlenburg & Babuška, 1995; Shen & Liu, 2007; Lourier et al., 2012).

20 Recently, data-driven methods using machine learning techniques have emerged as a new alternative  
21 in providing reliable solutions(Megalmani et al., 2021; Rao et al., 2017). However, there is always  
22 a possibility of contamination of measured data which affects the accuracy of the solution. Hence,  
23 there is need to develop methods that are driven by physics apart from the data(Raissi et al., 2019).  
24 Towards this direction, a neural network solution for the 1-D Helmholtz equation is presented in the  
25 current article.

26 According to universal approximation theorem, the solution of a well-posed problem can be approxi-  
27 mated to a desired accuracy with a feedforward neural network of infinite number of neurons(Hornik  
28 et al., 1989). Using this fact, a feedforward neural network is constructed to approximate the 1-D  
29 acoustic field. Unlike other governing equations, Helmholtz equation encounters biasing problem  
30 between the loss functions at higher frequencies(Wang et al., 2021). This problem can be bypassed  
31 by introducing unequal weights to the loss functionsMaddu et al. (2022); Basir & Senocak (2022).  
32 In this current article, an algorithm that automatically adjust the weights based on the calculated loss  
33 functions is proposed. Section 2 describes the neural network formulation for the 1-D Helmholtz  
34 equation. Problems associated with the higher frequencies, algorithm implementation to address  
35 this issue, and correlation with the true solution are presented in detail in Section 3. The article is  
36 concluded with final remarks in Section 4.

## 37 2 NEURAL NETWORK FORMULATION FOR THE 1-D HELMHOLTZ EQUATION

38 In many engineering applications such as human speech synthesis, automotive intake/exhaust sys-  
39 tems, HVAC ducts, etc., the acoustic field variation is primarily dominated in the direction of longest  
40 dimension. The acoustic field in that direction can be obtained by solving 1-D Helmholtz equation

41 given below(Munjaj, 2014)

$$\left(\frac{d^2}{dx^2} + k^2\right)\psi(x) = 0, \quad x \in [0, L] \tag{1}$$

42 subjected to the boundary conditions  $\psi(0) = \psi_0$  and  $\psi(L) = \psi_L$ . Here,  $\psi(x)$  is the acoustic field,  
 43  $k = 2\pi f/c$  is the wavenumber,  $f$  is the frequency and  $c$  is the speed of sound in air (340 m/s).

44 According to the universal approximation theorem(Hornik et al., 1989), the acoustic field  $\psi(x)$  can  
 45 be approximated with a feedforward neural network  $\hat{\psi}(x; \theta)$  and can be estimated by minimizing  
 46 the following loss functional  $\mathcal{L}$  with respect the parameters  $\theta$ (Raissi et al., 2019).

$$\mathcal{L}(\theta) = \mathcal{L}_F(\theta) + \mathcal{L}_B(\theta), \tag{2}$$

47 where  $\mathcal{L}_F(\theta)$  is the loss functions associated with the Helmholtz equation

$$\mathcal{L}_F(\theta) = \frac{1}{N} \sum_{i=1}^N \left\| \frac{d^2}{dx^2} \hat{\psi}(x^{(i)}; \theta) + k^2 \hat{\psi}(x^{(i)}; \theta) \right\|_2^2, \tag{3}$$

48 and  $\mathcal{L}_B(\theta)$  is the loss functions associated with the boundary conditions

$$\mathcal{L}_B(\theta) = \frac{1}{2} \left( |\hat{\psi}(0; \theta) - \psi_0|^2 + |\hat{\psi}(L; \theta) - \psi_L|^2 \right). \tag{4}$$

49 Here,  $N$  is the number of internal collocation points in  $[0, L]$ .

50 **3 RESULTS AND DISCUSSION**

51 A feedforward neural network with 4 hidden layers and 90 neurons in each layer is constructed to  
 52 predict the acoustic field  $\psi$ . The loss functional  $\mathcal{L}$  is optimised using *Adam* algorithm with *tanh*  
 53 activation function. The domain is divided into 10000 random collocation points and 10000 full-  
 54 batch iterations were performed with a learning rate of  $10^{-3}$ .

55 Figure 1 shows the acoustic field predicted by the neural network against the true solution obtained  
 56 from the analytical method (refer Appendix A) for different frequencies. It can be observed that the  
 57 neural network is able to learn the underlying physics from the governing equations successfully at  
 58 lower frequencies (100 Hz). At higher frequencies (above 200 Hz), there is a drastic deviation from  
 59 the true solution. The reason for this behaviour can best be understood by observing the variation of  
 individual loss functions with respect to iterations.

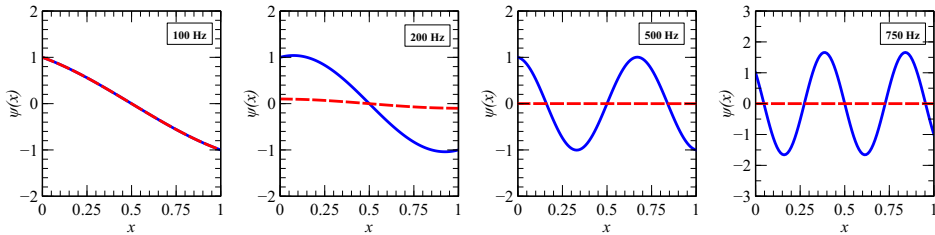


Figure 1: Correlation between true (—) and predicted solution (- - -) for different frequencies.

60

61 Figure 2 shows the variation of the loss functions  $\mathcal{L}_F$ ,  $\mathcal{L}_B$  and  $\mathcal{L}$  with respect to iteration for different  
 62 frequencies. It can be observed that both the loss functions decreases with respect to iterations at  
 63 lower frequencies (100 Hz). However, at higher frequencies (200 Hz and above), the loss function  
 64 associated with the Helmholtz equation  $\mathcal{L}_F$  decreases, whereas the loss function associated with the  
 65 boundary conditions  $\mathcal{L}_B$  does not decrease and becomes stable at particular value.

66 In other words, a biasing behaviour is introduced during the training process at higher frequencies,  
 67 which enforces the optimization process to favour  $\mathcal{L}_F$  alone and minimises it, leaving  $\mathcal{L}_B$ . This  
 68 problem can be bypassed by assigning weights to the loss functions as given below

$$\mathcal{L} = \lambda_F \mathcal{L}_F + \lambda_B \mathcal{L}_B, \tag{5}$$

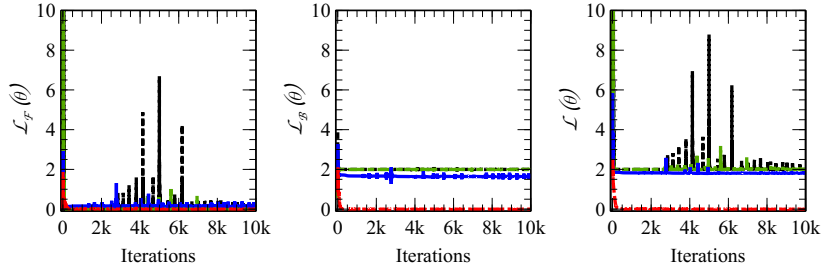


Figure 2: Variation of the loss functions with respect to the iterations: - - - 100 Hz, — 200 Hz, - · - · 500 Hz, · · · · 750 Hz.

69 where  $\lambda_F$  and  $\lambda_B$  are the weights associated with the loss functions  $\mathcal{L}_F$  and  $\mathcal{L}_B$ , respectively.

70 One of the simplest method to find  $\lambda_F$  and  $\lambda_B$  is to choose them on the trial-and-error basis method.  
 71 Even though this method is relatively easy, finding appropriate weights for each frequency makes  
 72 it cumbersome. In addition, any change in the boundary conditions will alter the problem and  
 73 the procedure needs to be repeated. Therefore, there is a need to develop an automatic weight  
 74 update procedure that guarantees the correlation for the chosen frequency range and the boundary  
 75 conditions. In the current work, an automatic weight update algorithm that works on the values of  
 76 the loss functions is proposed. In this algorithm  $\lambda_F$  is chosen as unity and  $\lambda_B$  is updated with each  
 iteration as follows

---

**Algorithm:** Training algorithm to update weights

---

```

Input:  $E$  // Input number of iterations
 $\lambda_F, \lambda_B \leftarrow 1$  // Initialize weights
 $\beta \leftarrow 10^{-3}$  // Assign hyperparameter
 $\epsilon \leftarrow 10^{-3}$  // Assign tolerance for the weight update

for  $iter$  1 to  $E$  do
  if  $\mathcal{L}_F/\lambda_B \leq \epsilon$  then
     $\hat{\lambda}_B \leftarrow 1$ 
  else
     $\hat{\lambda}_B \leftarrow \mathcal{L}_B/\mathcal{L}_F/\epsilon$  // Update intermediate weight
  end
   $\lambda_B \leftarrow (1 - \beta)\lambda_B + \beta\hat{\lambda}_B$  // Update weight associated with boundary loss
end

```

---

77

78 Figure 3 shows the comparison of results obtained with the weight update algorithm and the true  
 79 solution. It can be observed that a good correlation has been achieved by updating the weights  
 80 based on the loss functions. In other words, the algorithm is able to avoid the biasing behaviour of  
 81 the training process and is helping to optimise both the loss functions simultaneously. This can be  
 82 confirmed from the loss function plots draw in Fig. 4 with the automatic weight update algorithm.

83 Figure 4 shows the loss functions with respect to iterations for various frequencies. It can be ob-  
 84 served that unlike with the case of equal weights,  $\mathcal{L}_B$  with the weight update algorithm starts reduc-  
 85 ing with respect to iterations at higher frequencies. This ensures the neural network to learn physics  
 86 properly from the Helmholtz equation as well as the boundary conditions.

87 Table 1 shows the percentage of relative error between the prediction solution and the true solution  
 88 calculated as per Eq. (6) at different frequencies using the two methods

$$\% Error = \frac{\|\hat{\psi}_t(x; \theta) - \psi(x)\|_2}{\|\psi(x)\|_2} \times 100. \quad (6)$$

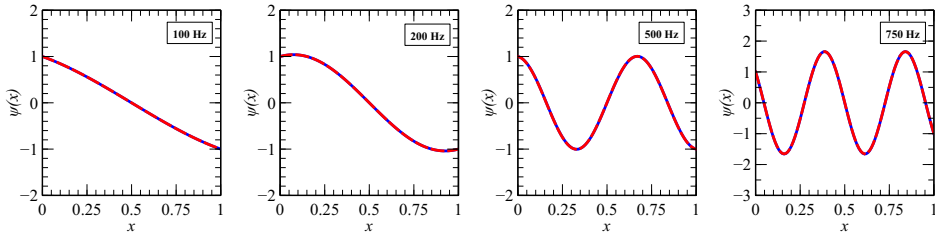


Figure 3: Correlation between true (—) and predicted solution (---) for different frequencies.

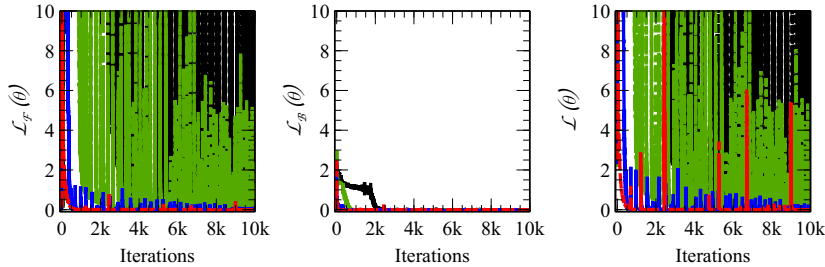


Figure 4: Variation of the loss functions with respect to the iterations: --- 100 Hz, — 200 Hz, -.- 500 Hz, ..... 750 Hz.

Table 1: Comparison of relative error (in percentage) at different frequencies.

Frequency (Hz)	Equal weights	Weight update
100	0.03	0.02
200	91.08	0.01
500	99.99	0.58
750	100	0.31

89 The weight update algorithm significantly reduces the error at higher frequencies and ensures proper  
 90 correlation with the true solution.

91 **4 CONCLUSION**

92 The acoustic field in a 1-D duct is estimated using neural network by posing the problem of govern-  
 93 ing differential equations as an unconstrained optimization problem with two loss functions. One  
 94 associated with the Helmholtz equation and the other associated with the boundary conditions. The  
 95 results reveal that at higher frequencies, the training process exhibits biasing behaviour. The opti-  
 96 mization process favours the loss function associated with the Helmholtz equation, and leaves that  
 97 associated with the boundary conditions. This problem is bypassed by introducing weights which  
 98 adjust their values based on the individual loss functions. The proposed automatic weight update al-  
 99 gorithm ensures the boundary loss to converge with respect to the iterations and helps the network to  
 100 learn the underlying physics properly. Quantitatively, the proposed algorithm keeps the relative error  
 101 to a maximum value of 0.58% within the frequency range considered for the analysis. The method  
 102 is having a potential to predict the acoustic field governed by the higher dimensional Helmholtz  
 103 equation as well as complicated boundary conditions and is need to be explored.

104 **REFERENCES**

105 S. Basir and I. Senocak. Physics and equality constrained artificial neural networks: application to  
 106 forward and inverse problems with multi-fidelity data fusion. *Journal of Computational Physics*,  
 107 463:111301, 2022.

- 108 K. Hornik, M. Stinchcombe, and H. White. Multilayer feedforward networks are universal approxi-  
109 mators. *Neural networks*, 2(5):359–366, 1989.
- 110 F. Ihlenburg and I. Babuška. Finite element solution of the helmholtz equation with high wave  
111 number part i: The h-version of the fem. *Computers & Mathematics with Applications*, 30(9):  
112 9–37, 1995.
- 113 J. M. Lourier, M. Di Domenico, B. Noll, and M. Aigner. Implementation of an efficient pressure-  
114 based cfd solver for accurate thermoacoustic computations. In *18th AIAA/CEAS Aeroacoustics  
115 Conference (33rd AIAA Aeroacoustics Conference)*, pp. 2089, 2012.
- 116 S. Maddu, D. Sturm, C. L. Müller, and I. F. Sbalzarini. Inverse dirichlet weighting enables reliable  
117 training of physics informed neural networks. *Machine Learning: Science and Technology*, 3(1):  
118 015026, 2022.
- 119 D. R. Megalmani, B. G. Shailesh, A. Rao, S. S. Jeevanavar, and P. K. Ghosh. Unsegmented heart  
120 sound classification using hybrid cnn-lstm neural networks. In *2021 43rd Annual International  
121 Conference of the IEEE Engineering in Medicine & Biology Society (EMBC)*, pp. 713–717. IEEE,  
122 2021.
- 123 M. L. Munjal. *Acoustics of Ducts and Mufflers, 2 ed.,.* John Wiley and Sons Ltd, 2014.
- 124 M. Raissi, P. Perdikaris, and G. E. Karniadakis. Physics-informed neural networks: A deep learn-  
125 ing framework for solving forward and inverse problems involving nonlinear partial differential  
126 equations. *Journal of Computational physics*, 378:686–707, 2019.
- 127 M. V. A. Rao, N. K. Kausthubha, S. Yadav, D. Gope, U. M. Krishnaswamy, and P. K. Ghosh.  
128 Automatic prediction of spirometry readings from cough and wheeze for monitoring of asthma  
129 severity. In *2017 25th European Signal Processing Conference (EUSIPCO)*, pp. 41–45. IEEE,  
130 2017.
- 131 L. Shen and Y. J. Liu. An adaptive fast multipole boundary element method for three-dimensional  
132 acoustic wave problems based on the burton–miller formulation. *Computational Mechanics*, 40:  
133 461–472, 2007.
- 134 D. Veerababu and B. Venkatesham. Green’s function approach for the transmission loss of con-  
135 centric multi-layered circular dissipative chamber. *The Journal of the Acoustical Society of  
136 America*, 147(2):867–876, 2020.
- 137 D. Veerababu and B. Venkatesham. A green’s function solution for acoustic attenuation by a cylin-  
138 drical chamber with concentric perforated liners. *Journal of Vibration and Acoustics*, 143(2),  
139 2021.
- 140 S. Wang, Y. Teng, and P. Perdikaris. Understanding and mitigating gradient flow pathologies in  
141 physics-informed neural networks. *SIAM Journal on Scientific Computing*, 43(5):A3055–A3081,  
142 2021.

## 143 A ANALYTICAL SOLUTION

144 The analytical solution for the 1-D Helmholtz equation

$$\left(\frac{d^2}{dx^2} + k^2\right)\psi(x) = 0, \quad x \in [0, L] \quad (7)$$

145 subjected to the boundary conditions

$$\psi(0) = \psi_0; \quad \psi(L) = \psi_L \quad (8)$$

146 can be obtained by assuming a solution of the form

$$\psi(x) = Ce^{\gamma x}, \quad (9)$$

147 where  $C$  and  $\gamma$  are the constants.

148 Upon substituting Eq. (9) in Eq. (7) yields the general solution

$$\psi(x) = C_1 \cos(kx) + C_2 \sin(kx). \quad (10)$$

149 By substituting the boundary conditions, the constants  $C_1$  and  $C_2$  can be evaluated and the actual  
150 solution can be written as

$$\psi(x) = \psi_0 \cos(kx) + \left[ \frac{\psi_L - \psi_0 \cos(kL)}{\sin(kL)} \right] \sin(kx). \quad (11)$$